Amyloid Beta42 oligomers up-regulate the excitatory synapses by potentiating presynaptic release while impairing postsynaptic NMDA receptors

The Journal of Physiology

https://jp.msubmit.net

JP-RP-2019-279345

Title: Abeta42 oligomers up-regulate the excitatory synapses by potentiating presynaptic release while impairing postsynaptic NMDA receptors

Authors: Andrea Marcantoni
Sabina Cerullo
Pol Buxeda
Giuseppe Chiantia
Valentina Carabelli
Emilio Carbone

Author Conflict: No competing interests declared

Author Contribution: Andrea Marcantoni: Conception or design of the work; Acquisition or analysis or interpretation of data for the work; Drafting the work or revising it critically for important intellectual content; Final approval of the version to be published; Agreement to be accountable for all aspects of the work Sabina Cerullo: Acquisition or analysis or interpretation of data for the work; Final approval of the version to be published; Agreement to be accountable for all aspects of the work Pol Buxeda: Acquisition or analysis or interpretation of data for the work; Final approval of the version to be published; Agreement to be accountable for all aspects of the work Giuseppe Chiantia: Acquisition or analysis or interpretation of data for the work; Final approval of the version to be published; Agreement to be accountable for all aspects of the work Valentina Carabelli: Drafting the work or revising it critically for important intellectual content; Final approval of the version to be published; Agreement to be accountable for all aspects of the work Emilio Carbone: Drafting the work or revising it

critically for important intellectual content; Final approval of the version to be published; Agreement to be accountable for all aspects of the work

Running Title: Neuronal dysfunctions induced by Abeta42 oligomers

Dual Publication: No

Funding: MIUR: Valentina Carabelli, 2015FNWP34; Compagnia San Paolo: Valentina Carabelli, CSTO165284; MIUR: Andrea Marcantoni, FFABR AM received local funds from Torino University assigned without a reference number

Abeta42 oligomers up-regulate the excitatory synapses by potentiating presynaptic release while impairing postsynaptic NMDA receptors

Andrea Marcantoni[1*], Maria Sabina Cerullo[1, 2], Pol Buxeda[1], Giuseppe Chiantia[1], Valentina Carabelli[1], Emilio Carbone[1]

[1]*Department of Drug Science and Technology, Torino University (Italy)*

[2] *Center for Synaptic Neuroscience and Technology, Istituto Italiano di Tecnologia, Largo Rosanna Benzi 10, 16132 Genova,(Italy)*

**Address correspondence to*: Andrea Marcantoni,

Department of Drug Science and Technology,

Torino University

Corso Raffaello 30 10125 Torino, Italy.

Telephone: +39 0116708312

Fax: +390116708498

Email: andrea.macantoni@unito.it

Running title: Neuronal dysfunctions induced by Abeta42 oligomers

Keywords: NMDA receptors (NMDARs), Abeta42, synapses, calcium, ryanodine receptors (RyRs), dantrolene

Author profile

Andrea Marcantoni got his PhD in Physiology in 2004. During his post-doc period he mainly worked on the Ca^{2+}-dependent modulation of various cellular functions. As a tenure-track researcher at the Department of Drug Science and Technology (DSTF) in Torino (Italy), in the last five years AM concentrated his interests on the role of voltage-gated Ca^{2+} channels on cell firing and neurotransmitter release in neurons and neuroendocrine cells. He currently works on the pathological effects of amyloid beta peptides accumulation on hippocampal neurons by focusing on their ability to induce Ca^{2+} dysregulation and impaired neuronal excitability and synaptic plasticity. AM is now associate professor at the DSTF in Torino (Italy).

Key point summary

- NMDA receptors (NMDARs) are key molecules for controlling neuronal plasticity, learning and memory processes. Their function is impaired during Alzheimer's disease (AD) but the exact consequence on synaptic function is not yet fully identified.
- An important hallmark of AD onset is represented by the neuronal accumulation of Amyloid Beta42 oligomers (Abeta42) that we have recently shown to be responsible for the increased intracellular Ca2+ concentration through Ryanodine Receptors (RyRs)
- Here we characterized the effects of Abeta42 oligomers on NMDA synapses showing specific pre- and post-synaptic functional changes that lead to a potentiation of basal and synchronous NMDA synaptic transmission.
- These overall effects can be abolished by decreasing Ca2+ release from RyRs with specific inhibitors that we propose as new pharmacological tools for AD treatment.

Abstract

We have recently shown that Abeta42 oligomers (Abeta42) cause calcium dysregulation in hippocampal neurons by stimulating Ca^{2+} release from ryanodine receptors (RyRs) and inhibiting Ca^{2+} entry through NMDA receptors (NMDARs). Here, we found that Abeta42 decreases the average NMDA-activated inward current and that Ca^{2+}-entry through NMDARs is accompanied by Ca^{2+} release from the stores. The overall amount of $[Ca^{2+}]_i$ increase during NMDA application is 50% associated to RyRs opening and 50% to NMDARs activation. Addition of Abeta42 does not change this proportion. We estimated the number of NMDARs expressed in hippocampal neurons and their unitary current. We found that Abeta42 decreases the number of NMDARs without altering their unitary current. Paradoxically, the oligomer increases the size of electrically evoked eEPSCs induced by NMDARs activation. We found that this is the consequence of the increased

rate of glutamate release (p) and number of release sites (N) of NMDA synapses, while the quantal size (q) is significantly decreased as expected from the decreased number of NMDARs. An increased number of release sites induced by Abeta42 is also supported by the increased size of the *ready releasable pool* (RRP) and by the enhanced percentage of *paired pulse depression* (PPD). Interestingly, the RyRs inhibitor dantrolene prevents the increase of *PPD* induced by Abeta42 oligomers. In conclusion, Abeta42 up-regulates NMDA synaptic responses with a mechanism involving RyRs that occurs during the early stages of AD onset. This suggests that new selective modulators of RyRs may be useful for designing effective therapies to treat AD patients.

Introduction

Accumulation of amyloid beta (Abeta) oligomers derived from amyloid precursor protein (APP) processing induces neuronal Ca^{2+} dysregulation and synaptic dysfunction and is considered one of the better defined hallmarks of Alzheimer's disease (AD). Abeta oligomers cause dysregulation of Ca^{2+} homeostasis, neuronal cell death and consequent impairment of memory formation. Ca^{2+} dyshomeostasis induced by Abeta oligomers suggests some priority in the development of early strategies for the treatment of Ca^{2+}-mediated neuronal impairments. Uncontrolled increase of intracellular Ca^{2+} concentration ($[Ca^{2+}]_i$) may result from the alteration of different pathways of Ca^{2+} entry through the plasma membrane or Ca^{2+} release from Ca^{2+} stores. During the past fifteen years, data have been accumulated concerning the impairment of both mechanisms of $[Ca^{2+}]_i$ increase during AD. Specifically, Abeta oligomers affect Ca^{2+} entry through NMDARs (Snyder *et al.*, 2005; Zhang *et al.*, 2016) and/or voltage-gated calcium channels (VGCCs) (Nimmrich *et al.*, 2008; Thibault *et al.*, 2012; Wang & Mattson, 2013).

NMDARs are key regulators of memory formation (Costa *et al.*, 2012). They are upregulated during AD onset, causing increased $[Ca^{2+}]_i$ (Danysz & Parsons, 2012), impaired synaptic function and accelerated neuronal death. VGCCs are also targeted by Abeta oligomers, but opposite evidence suggests either an up- or down-regulation depending on the experimental procedure and brain region considered (Thibault *et al.*, 2012; Wang & Mattson, 2013). The alternative mechanism of $[Ca^{2+}]_i$ increase associated with RyRs and IP_3 receptors (IP_3Rs) activation is impaired during AD onset (Mattson, 2010). RyRs and IP_3Rs are not equally distributed along the ER membrane. IP_3Rs are preferentially located in the somatic region and possibly involved in the control of Ca^{2+}-dependent excitatory phenomena while RyRs are preferentially expressed in the ER close to the synaptic sites (Chakroborty *et al.*, 2013) and likely involved in the control of $[Ca^{2+}]_i$ governing synaptic activity. Our present goal on synaptic dysfunction induced by Abeta42 and associated with the functional coupling of RyRs to IP_3Rs (Berridge, 2011), RyRs to NMDARs (Goussakov *et al.*, 2010) and VGCCs (Kim *et al.*, 2007), is primarily focused on the RyRs impairment induced by Abeta oligomers during AD onset.

We have previously observed that spontaneous firing and intracellular Ca^{2+} homeostasis of hippocampal neuronal network was altered after incubation with Abeta42 and concluded that a target of Abeta42 is the postsynaptic NMDAR activity (Gavello et al., 2018). Starting from these considerations, here we performed patch-clamp and Ca^{2+} imaging recordings to test how the neurotoxic oligomer acts on NMDA-type glutamatergic synapses. We found that Abeta42 alters NMDA synapses by differently targeting pre and postsynaptic sites. In particular, we found that

Abeta42 reduces the number of postsynaptic NMDARs without altering their unitary current. These inhibitory effects contrast with the presynaptic potentiating action of Abeta42 that produces intracellular calcium transient increases (Gavello et al. 2018) that can account for the increased eEPSCs amplitude during asynchronous spontaneous firing or electrical stimulation. Using *multiple probability fluctuation analysis* (MPFA) we next observed that Abeta42 increases both the release probability (p) and the number of release sites (N) of NMDA synapses, justifying the enhanced NMDA-mediated eEPSCs amplitude. In line with this, through the analysis of cumulative eEPSCs during high frequency stimulation (10 Hz) we found that Abeta42 increases the size of the ready-releasable pool (RRP). Interestingly, administration of RyRs inhibitor dantrolene restores p and the size of eEPSCs to control values, suggesting that RyRs play a key role in the altered mechanisms of NMDA-type synaptic transmission induced by Abeta42. In conclusion, our data prompt a valuable description of how Abeta42 up-regulates NMDA synaptic responses with a mechanism involving RyRs (Danysz & Parsons, 2012) during the early stages of AD onset. This also suggests that selective modulators of RyRs may be potential new drugs to treat AD patients.

Methods

Ethical approval

Ethical approval was obtained for all experimental protocols from the University of Torino Animal Care and Use Committee, Torino, Italy. All experiments were conducted in accordance with the National Guide for the Care and Use of Laboratory Animals adopted by the Italian Ministry of Health. All animals had free access from the shelter to water and food. Every effort was made to minimize animal suffering and the number of animals used. For removal of tissues, animals were deeply anaesthetized with CO2 inhalation at fixed concentration and rapidly killed by cervical dislocation.

Cell culture

All experiments were performed in accordance with the guidelines established by the National Council on Animal Care and approved by the local Animal Care Committee of Turin University. Hippocampal neurons were obtained from C57BL/6 mouse 18-day embryos. Hippocampus was rapidly dissected under sterile conditions, kept in cold HBSS (4ºC) with high glucose, and then digested with papain (0.5 mg/ml) dissolved in HBSS plus DNAse (0.1 mg/ml) as previously described (Allio *et al.*, 2015). Isolated cells were plated at the final density of 1200 cells/mm^2. Recordings were carried out at DIV 18.

Patch Clamp experiments

Patch electrodes, fabricated from thick borosilicate glasses (Hilgenberg, Mansifield, Germany), were pulled to a final resistance of 3-5 MΩ. Patch Clamp recordings were performed in whole cell configuration using a Multiclamp 700-B amplifier connected to a Digidata 1440 and governed by the pClamp10 software (Axon Instruments, Molecular Devices Ltd, USA).

Experiments were performed at room temperature (22-24 °C) in whole cell configuration and acquired with sample frequency of 10 KHz. eEPSCs were filtered at half the acquisition rate with 8-pole low-pass Bessel filter. Recording with leak current >100pA or series resistance >20MΩ were discarded. Analysis was performed with Clampfit software (Axon Instruments). Noise analysis on mEPSCs was performed with MiniAnalysis software (Synaptosoft, USA). Data are expressed as means ± S.E.M and statistical significance was calculated by using Student's t-test. Values of $p < 0.05$ were considered significant.

Voltage clamp

For currents dependent by NMDA administration, recording neurons were hold at -70mV (V_h) for the entire duration of the experiments.

NMDA dependent EPSCs following spontaneous APs or electrical stimulation were recorded by holding neurons at voltages comprised between -70mV and +50mV. eEPSCs were recorded by delivering presynaptic electrical stimuli through a glass pipette (1 μm tip diameter) filled with Tyrode's solution and placed in contact with the soma of presynaptic neuron in a loose-seal configuration. The minimum amplitude (10–45 μA) of current pulses of 0.1 ms duration was generated by an isolated pulse stimulator (model 2100; A-M Systems, USA). Postsynaptic neurons were hold at potentials comprised between -70 and + 50mV according to the typology of the experiment.

Calcium imaging

Hippocampal neurons plated on glass petri dishes were loaded with the fluorescent Ca^{2+} indicator Fura2-AM dye (3 μM) (Invitrogen, Molecular Probes, USA) in the extracellular solution for 1 hour. The fluorescent dye was then washed, and extracellular solution containing picrotoxin (100μM) was replaced into the petri dish. The inverted microscope used (Leica DMI3000B, Germany) was equipped with a short-arc xenon gas discharge lamp (Ushio, Cypress, USA). Alternating excitation wavelengths of 340 nm and 380 nm were obtained by a monochromator (Till Photonics, Germany). The emitted fluorescence was measured at 500-530 nm. Images were projected onto a EMCCD camera (QuantEM:512SC, Photometrics, USA) and stored every 200 ms. Spontaneous Ca^{2+} transients were recorded both in control condition and after incubation with Abeta42 using Metafluor software (Molecular Devices, USA) for data acquisition. The relative change in fluorescence ($\Delta F/F$) was measured considering the peak of Ca^{2+} transients.

Solutions and drugs

For voltage clamp recordings the external solution contained (in mM): 130 NaCl, 1.8 CaCl2, 10 HEPES, 10 glucose, 1.2 Glicine (pH 7.4). The internal solution contained (in mM): 90 CsCl, 8 NaCl, 20 TEACl, 10 EGTA, 10 Glucose, 1 MgCl, 4 ATP, 0.5 GTP, 15 Phosphocreatine (pH 7.4 with CsOH). For blocking synaptic currents due to the activation of glutamatergic AMPARs and GABAergic synapses (GABAA receptors) we added respectively 6,7-dinitroquinoxaline-2,3-dione, DNQX (20 μM, Sigma-Aldrich, USA) and picrotoxin (100 μM, Sigma-Aldrich). Tetrodotoxin (TTX 0.3 μM, Tocris Bioscience, UK) was added to block voltage-gated Na+ channels. Dantrolene (10 μM, Sigma-Aldrich) was added to block RyRs. (2R)-amino-5-phosphonopentanoate, APV (50 μM, Sigma Aldrich) was added for blocking NMDARs.

Statistics

Data are given as mean ± SEM for *n* number of cells. Statistical significance was estimated using either paired or unpaired Student's *t*. Data were found statistically significant when $P < 0.05$.

Results

Abeta42 oligomers decrease NMDAR inward currents without impairing ligand-receptor binding affinity

Networks of primary cultured hippocampal neurons are known to generate spontaneous bursts of action potentials (APs) (Bacci *et al.*, 1999; Gavello *et al.*, 2012) that are modulated by inhibitory and excitatory synapses (Gavello *et al.*, 2018). Glutamatergic synapses dependent on NMDARs activation (NMDA-driven synapses), are involved in the modulation of spontaneous network excitability and inhibited by Abeta42 oligomers (Gavello *et al.*, 2018). As a first approach, we tested whether this inhibition affected pre or postsynaptic mechanisms. To this purpose, we compared NMDA-activated currents in control versus Abeta42-treated neurons. Patch clamp experiments, performed by holding neurons at V_h= -70 mV, showed that 50 μM NMDA induces a mean inward current of 352 ± 3 pA (n= 31) through NMDARs (I_{NMDA}) that is reduced to 117 ± 15 pA (n= 23) by 1 μM Abeta42 (*** $p<0.001$) (Fig. 1a-c). Comparable decreases were obtained by varying NMDA concentration from 20 to 300 μM (Fig. 1c) or by decreasing the Abeta42 concentration to 10 nM. Under this condition (not shown), we still observed that 10 nM Abeta42 reduced I_{NMDA} by 30% with 50 μM NMDA (from 711 ± 79 pA, n= 17, to 487 ± 78 pA, n=15; $p<0.05$). Plots of I_{NMDA} versus [NMDA] (from 2 to 300 μM) exhibited dose-response relationship fitted by Hill equations of similar steepness (*p*) and IC_{50} (see Fig. 1d legend). The *p* values were

1.4±0.4 μM in control (ctr) and 1.5±0.4 μM in the presence of Abeta42 and the IC_{50} were 17.3 ± 3.3 μM in control and 16.5±3.9 μM with Abeta42 (Fig. 1d). We thus concluded that Abeta42 inhibits the I_{NMDA} amplitude without significantly affecting the stoichiometry and the ligand-receptor binding affinity.

Abeta42 decreases the number of NMDARs without altering their single channel conductance

In order to understand how Abeta42 inhibits postsynaptic NMDA-activated currents we estimated the mean number of functioning NMDARs and their single channel conductance both in control and in the presence of Abeta42, by comparing the variance (σ^2) of I_{NMDA} stationary noise (Sigworth, 1980). We calculated σ^2 for periods of 2 s during stationary conditions of I_{NMDA} and plotted the values as a function of the average I_{NMDA} amplitudes generated by increased concentrations of NMDA (Traynelis & Jaramillo, 1998). The relationship between σ^2 and I_{NMDA} is described by the following parabolic equation: $\sigma^2 = iI - I^2/n$, where *i* is the unitary current of NMDARs, *n* the number of activated NMDARs and *I* the mean I_{NMDA} amplitude. We observed drastic lower values of I_{NMDA} amplitudes and σ^2 in neurons incubated with Abeta42 compared to control neurons (Fig. 2a-d). The fit with the above parabolic function gave a significantly decreased number of NMDARs (*n*) with Abeta42 (from 455 ± 66 to 249 ± 44 after incubation with Abeta42; *p<0.05) (Fig. 2e) and nearly similar values for the single channel unitary current (*i*) (1.9 ± 0.2 pA in control neurons and 1.8 ± 0.2 pA in cells treated with Abeta42) (Fig. 2f). The corresponding single channel conductance of NMDARs were 19 and 20 pS, respectively in controls and Abeta42-treated neurons calculated assuming a reversal potential (V_{rev}) of +25 mV that was determined from the reversal potential of mEPSCs (Fig. 5a). Finally, we estimated the maximum open probability of NMDAR channels $p = N/i$ (Traynelis & Jaramillo, 1998) and found no significant changes (p=0.83) between control (0.50 ± 0.05) and Abeta42 treated neurons (0.52 ± 0.06) (Fig. 2g).

Abeta42 oligomers decrease $[Ca^{2+}]_i$ but preserve the Ca^{2+}-induced Ca^{2+} release coupling between NMDARs and RyRs

Having previously shown that Abeta42 increases the amount of $[Ca^{2+}]_i$ by targeting RyRs (Gavello *et al.*, 2018), we wondered whether NMDARs, known to be permeable to Ca^{2+} (Emptage *et al.*, 1999), were involved in this process. Using Ca^{2+} imaging we quantified the $[Ca^{2+}]_i$ increase induced by NMDA administration (50 μM) and its modulation by Abeta42, knowing that the mechanism of Ca^{2+}-induced Ca^{2+} release (CICR) through RyRs activation is upregulated by Abeta42 (Gavello *et al.*, 2018). We observed a marked increase of $[Ca^{2+}]_i$ during NMDA application (Fig. 3a) that was fully abolished in the absence of extracellular Ca^{2+}. In control neurons (Fig. 3b), NMDA induced an

approximately 8-fold increase of $[Ca^{2+}]_i$ ($\Delta F/F = 7.9 \pm 1.2$, n= 25) that was nearly halved by Abeta42 ($\Delta F/F = 4.7 \pm 0.4$, n= 33; *p<0.05) (Fig. 3b-e).

To quantify the involvement of RyRs in the CICR mechanism triggered by NMDA, we inhibited RyRs by applying 10 μM dantrolene (Zhao *et al.*, 2001). Surprisingly enough, in control and Abeta42-treated neurons dantrolene reduced to nearly half the NMDA-induced $[Ca^{2+}]_i$ increase. $\Delta F/F$ decreased from 7.9±1.2 to 3.7±0.6 (n=33; **p<0.01) in control (Fig.3 b, d) and from 4.7±0.4 to 2.4±0.3 (n=31;***p<0.001) (Fig. 3c,e) in Abeta42-treated neurons. These results confirm that the NMDA-mediated $[Ca^{2+}]_i$ increase is nearly half associate to a CICR mechanism that involves RyRs and that this mechanism is not impaired by Abeta42. In fact, the $[Ca^{2+}]_i$ increase associated to the RyRs is 40% of the total in control and raises to 49% with the oligomers. In addition, since Abeta42 induces a potentiating effect on the Ca^{2+} released from RyRs, it is evident that the Abeta42 prevailing effect is an overall decrease of the amount of $[Ca^{2+}]_i$ following NMDARs activation.

Abeta42 does not affect the number of release sites of NMDA-regulated synapses

To gain further insights on the effects of Abeta42 on glutamatergic NMDA synapses, we measured the eEPSCs amplitude by holding neurons at +20 mV and varying the extracellular concentration of $CdCl_2$ (6 to 2 μM) and $CaCl_2$ (2 to 5 mM) to increase the release probability and thus increasing eEPSCs amplitudes (Fig. 4a) (Clements & Silver, 2000). By comparing the eEPSCs amplitudes (Fig. 4a,c,e) with those measured in neurons incubated with Abeta42 (Fig.4b,d,f), we found that the oligomer significantly increased the mean eEPSC amplitude (from 241 ± 27 pA, n=14, to 344 ± 40 pA, n=19, * p<0.05, in the presence of 2 mM $CaCl_2$) (Fig. 4g). We next performed *multiple probability fluctuation analysis* (MPFA) to estimate the number of release sites (N), the quantal size (q) and the release probability (p) of glutamatergic NMDA synapses (Silver *et al.*, 1998; Clements & Silver, 2000; Baldelli *et al.*, 2005). A parabolic function ($\sigma^2 = AI_{av} - BI_{av}^2$) describes the relationship between the variance of eEPSCs amplitude (σ^2) and their mean postsynaptic current amplitude values (I_{av}) (Fig. 4c, d). N was obtained from B ($N = 1/B$), while q was taken equal A. Finally, p was estimated considering that $I_{av} = N\,p\,q$. We observed that with Abeta42 N increased significantly from 137 ± 39 to 267 ± 51 (*p<0.05) (Fig. 4h), while q decreased from 6.1 ± 0.8 pA to 4.0 ± 0.6 pA (*p<0.05) (Fig. 4i) and p, measured in 2 mM $CaCl_2$, increased from 0.2 ± 0.02 to 0.3 ± 0.03 (*p< 0.05). Thus, MPFA suggests that Abeta42 increases the number of release size while decreasing the quantal size of release. We next focused on the presynaptic effects of Abeta42, possibly responsible for the observed increased rate of glutamate release and in turn for the increased p as well as eEPSC amplitude.

Abeta42 increases the amplitude and frequency of spontaneous EPSCs

Since spontaneous firing of hippocampal neurons is impaired by Abeta42 and NMDARs is involved in this process (Gavello *et al.*, 2018), we next determined how the oligomers affect the amplitude and frequency of EPSCs generated at NMDA synapses during spontaneous APs at V_h varying from -70 to +50 mV. The EPSCs reversal potential was between +20 and + 30 mV and Abeta42 increased significantly the average EPSCs amplitude at every potential (Fig. 5a-c). At V_h= -70 mV the average EPSCs amplitude in control neurons was -403 ± 65 pA (n=7), while in the presence of Abeta42 it increased to -826 ± 83 pA (n=13;** $p<0.01$) (Fig. 5a, inset). When the interevent intervals (IEIs) were considered (Fig. 5d,e), they were shorter and more regular in Abeta42 treated neurons. IEIs in control and Abeta42-treated neurons had rather different Gaussian distributions. Control IEIs were best fitted with a double Gaussian function, with peaks respectively at 662.8 and 1841.3 ms (Fig. 5d), while IEIs in Abeta42-treated neurons were distributed according to a single Gaussian function with a peak at 1204 ms (Fig. 5e). The corresponding cumulative probability functions were significantly different (Kolmogrov Smirnov (KS) test ***$p<0.001$) (Fig. 5f) and the same was for the coefficient of variation (CV) of IEIs that decreased markedly in Abeta42-treated neurons (0.60 ± 0.03 in control neurons vs. 0.28 ± 0.03 with Abeta42; ***$p<0.001$) (Fig. 5g). Thus, Abeta42 besides increasing the EPSCs amplitude, increases their frequency and regularity of occurrence.

Abeta42 increases synaptic depression during trains of stimuli

To better analyze the effects of Abeta42 on synaptic function we next assayed the NMDA-mediated synaptic response to high frequency stimulation (10 Hz) for periods of 1.5 s (Schneggenburger *et al.*, 2002; Baldelli *et al.*, 2005). Following this protocol, the amplitude of the eEPSCs was maximal during the first pulse of the train and then progressively depressed until reaching a constant value during the last 5-6 pulses, when the eEPSC amplitude reaches steady-state conditions (Fig. 6a, top). There was no sign of facilitation both in control and in Abeta42-treated cells. Nevertheless, it was evident that the eEPSCs depression during the steady state phase was more pronounced in Abeta42-treated neurons, despite the size of the first eEPSC was higher than in control conditions (Fig.6a, bottom). The increased synaptic depression in Abeta42 treated neurons was clearly visible when the normalized amplitude of eEPSCs was plotted vs. time (Fig. 6b) and fitted by a double exponential function with fast (τ_f) and slow (τ_s) time constants. We observed that τ_f and τ_s decreased in the presence of Abeta42, respectively from 0.97 and 32 ms (in control) to 0.30 and 13.4 ms with Abeta42.

We next focused on the cumulative profile of eEPSC amplitudes observing in control and in Abeta42-treated neurons a rapid rise of cumulative eEPSCs followed by a steady-state linear

increase (Fig. 6c). This last linear phase reflects the equilibrium condition between vesicle release and vesicle replenishment. According to Schneggenburger et al, (2002) the intercept on the y-axis of the backward linear extrapolation of the last 5 to 6 points of the cumulative amplitude furnishes a likely estimate of the RRP size generating the eEPSCs. The linear fits of the cumulative amplitudes show clearly an increased size of RRP from 655 ± 143 pA (n=12) in control to 1040 ± 361 pA (n=11) in Abeta42-treated neurons (Fig. 6d). We could also estimate the release probability *p* that a vesicle is released from the RRP by calculating the ratio between the size of the first eEPSCs and the RRP and observed that Abeta42 significantly increased *p* from 0.67 ± 0.03 to 0.84 ± 0.08 (*p<0.05) (Fig. 6e).

Abeta42 oligomers increase the paired pulse depression of eEPSCs.

To elucidate the presynaptic mechanism responsible for the increased eEPSCs amplitude induced by Abeta42, we tested whether the Abeta42-mediated increase of EPSCs influences the probability of Ca^{2+}-dependent neurotransmitter release. We therefore estimated the percentage of *paired pulse depression* (PPD) of eEPSCs by electrically stimulating presynaptic neurons with pair of pulses separated by interpulse intervals of increasing duration (from 25 ms to 2 s) (Baldelli *et al.*, 2002). Percentage of PPD plotted versus the interpulse interval duration decreased following a double exponential decay both in control and in Abeta42-treated neurons (Fig. 7a). Within the first 100 ms the PPD decreased from 55.4 ± 3.6 % to 39.3 ± 4.0 % (n= 21) in control (Fig. 7c and inset in Fig. 7a), while in Abeta42 treated neurons it decreased from initial higher values: 72.8 ± 4.3 % to 52.8 ± 5.6 %, n=13; *p<0.05). At interpulse intervals longer than 100 ms, PPD decayed with a slower time constant that was not significantly different between control and Abeta42-treated neurons. Since the magnitude of PPD at very brief interpulse intervals approximates the probability of release (*p*) (Dittman & Regehr, 1998), we can conclude that Abeta42 acts presynaptically by increasing the probability of glutamate release.

When PPD was measured in the presence of dantrolene together with Abeta42, its amplitude and decay time were comparable to that measured in control neurons (Fig. 7b, e). This suggests that the increased probability of glutamate release with Abeta42 is most likely due to the amount of calcium released from RyRs that dantrolene effectively prevents. Finally, when comparing the average amplitude of the first eEPSC (Fig.7c, d) at V_h=-70 mV we could observe that Abeta42 causes a significant increase of the EPSC (from 320 ± 39 pA (n=13) to 466 ± 68 pA (n=9); *p<0.05), partially prevented by dantrolene (390 ± 65 pA, n=13, Fig. 7e).

Discussion

We provided evidence that Abeta42 impairs NMDAR-mediated glutamatergic synapses and targets both pre and postsynaptic sites. Abeta42 inhibits the average current amplitude generated by NMDARs activation by decreasing the number of postsynaptic NMDARs without altering their unitary current and open probability. These inhibitory postsynaptic effects decrease the amount of calcium entering into the cell through NMDARs and this apparently contrast with the previously reported increase of total Ca^{2+} released through RyRs induced by Abeta42 (Gavello *et al.*, 2018). To clarify this issue we focused on EPSCs elicited by presynaptic electric stimulation or spontaneous APs. We unmasked a dual effect of Abeta42 that should not be ignored in the development of new therapies for AD treatment presently focused exclusively on NMDA synapses and based on the inhibition of NMDARs (Folch *et al.*, 2017). We show that the postsynaptic inhibitory effect induced by Abeta42 on NMDA synapses opposes with the enhancing effect generated at the presynaptic site, where Abeta42 increases the eEPSCs amplitude by increasing the release probability of glutamate, the number of release sites and the size of the RRP of NMDA synapses. Finally, we have pointed out that RyRs inhibition restores the average amplitude of eEPSCs to values comparable to those measured in control neurons and abolishes the increased PPD induced by Abeta42. In agreement with our previous results (Gavello *et al.*, 2018), we confirm that inhibition of RyRs could be a promising strategy for treating early symptoms of AD.

Abeta42 decreases NMDA-activated inward current by reducing the number of postsynaptic NMDARs

To distinguish the pre and postsynaptic effects induced by Abeta42 on NMDA glutamatergic synapses, we first focused on the postsynaptic effects on NMDARs. The inward current amplitude estimated during NMDA application is smaller if compared to the size of spontaneous EPSCs activated by synchronous glutamate release (Fig. 1, 5). This is in good agreement with the well-known property that NAMDRs are more sensitive to glutamate than to NMDA (Monyer *et al.*, 1992). Given this, we have shown that, the oligomer decreases the expression of functionally active NMDARs without modifying the unitary current and open probability of the channel (Fig. 2). Interestingly, the estimated NMDARs single channel conductance (20 pS) appears comparable to that measured in *Xenopus* oocytes (ref) or obtained by using a similar approach (21-35 pS) (Kohr *et al.*, 1993) and is in reasonable agreement with that measured in single channel out-side-out patches of dissociated hippocampal neurons from neonatal rats (40-50 pS) (Jahr & Stevens, 1987; Bekkers & Stevens, 1989).

Our findings are also in line with the idea of a downregulation of the non amyloidogenic pathway of APP processing during AD (Snyder *et al.*, 2005; Shankar *et al.*, 2007) with consequent altered

synaptic plasticity and neuronal survival (Hoey *et al.*, 2009). The non amyloidogenic pathway is upregulated by Ca^{2+} entering through NMDARs and the decreased Ca^{2+} influx through these receptors induced by Abeta42 contributes to exacerbate the early impairments induced by the oligomer. Abeta oligomers cause the inhibition of LTP (Lambert *et al.*, 1998) and, given the importance of Ca^{2+} influx through NMDARs in modulating spine formation, the decreased Ca^{2+} influx through NMDARs and consequent reduction of spine density induced by the oligomers (Shankar *et al.*, 2007) are likely the triggering events of impaired learning and memory in AD. Here, we provide further explanation on the mechanism of action of Abeta42 on postsynaptic NMDARs in determining hippocampal synaptic dysfunction by reducing the expression density of these receptors.

Abeta42 decreases the amount of $[Ca^{2+}]_i$ triggered by NMDARs activation but preserves the Ca^{2+} induced-Ca^{2+} release coupling to RyRs

Our findings on the $[Ca^{2+}]_i$ increase induced by NMDA nicely correlate with patch clamp experiments and show that I_{NMDA} inhibition by Abeta42 is accompanied by a proportional decrease of the Ca^{2+} entering through NMDARs. In neurons, a CICR coupling that triggers Ca^{2+} release from the endoplasmic reticulum via RyRs and IP_3 receptors (Emptage *et al.*, 1999) accompanies this process. We aimed to correlate this result with our recently published findings on the overall increase of $[Ca^{2+}]_i$ induced by Abeta42 (Gavello *et al.*, 2018) and wondered whether the CICR coupling triggered by NMDARs was impaired by Abeta42. Our data indicate that, independently of the presence of Abeta42, Ca^{2+} released from RyRs account for half of the total $[Ca^{2+}]_i$ increase and concluded that Abeta42 does not interfere with this mechanism of CICR. We therefore suggest that differently from what previously observed by others (Goussakov *et al.*, 2010), Ca^{2+} released from RyRs following NMDARs activation is not responsible for the increased $[Ca^{2+}]_i$ induced by Abeta42, possibly reflecting the different experimental model used in the experiments. We suggest that other Ca^{2+} sources responsible for potentiating Ca^{2+} release from RyRs are likely to be involved, like the VGCCs that are downregulated by Abeta42 (Gavello *et al.*, 2018), or IP_3 receptors, known to be modulated by RyRs (Berridge, 2011) and to be impaired in some AD mouse model (Stutzmann *et al.*, 2004). Alternatively, the existence of calcium leak phenomena coupled to RyRs should also be considered (Lacampagne *et al.*, 2017).

Abeta42 increases the size of eEPSCs triggered by NMDARs activation

Using *multiple probability fluctuation analysis* (MPFA) (Clements & Silver, 2000) we could estimate the average number of synaptic release sites (N), the release probability (p) and the quantal size (q). Visual inspection of the shape of parabolic variance-mean plot (Clements & Silver, 2000)

reveals that the initial slope of the parabola is lowered by Abeta42 (Fig. 4), suggesting a decreased *q,* which is in line with the decreased number of NMDARs estimated in Abeta42-treated neurons. Moreover, the degree of curvature of the same parabola is higher in the presence of Abeta42, confirming the increased *p*. This is in line with the analysis of cumulative EPSCs (Fig. 6) and increased PPD (Fig. 7). Finally, Abeta42 increases the size of the parabola that depends on *N* (Fig. 4h).

In addition to this, voltage-clamp experiments provide evidence that, differently from what observed during direct application of NMDA (Fig. 1), neurons incubated with Abeta42 exhibit increased eEPSCs amplitude. This is at variance from what we observed on AMPA synapses (Gavello *et al.*, 2018) where eEPSCs amplitude are potentiated by Abeta42 only in the presence of RyRs or BK channels inhibitor indicating the existence of a "braking" action of calcium released from RyRs as already observed in 3xTg-AD mice (Chakroborty *et al.*, 2009). This suggests different effects induced by increasing release of Ca^{2+} from RyRs on AMPA or NMDA synapses and underlie the need of an in-depth characterization of synaptic dysfunctions induced by Abeta42. A potentiating effect of Abeta42 on the EPSCs size is also evident by observing the larger amplitude, higher frequency and increased regularity of spontaneous EPSCs in the presence of Abeta42 (Fig. 5). All this suggests that Abeta42 is likely responsible for a presynaptic Ca^{2+}-dependent potentiating effect of glutamatergic synapses. Of particular interest is the increased regularity of spontaneous EPSCs induced by Abeta42. To this regard, it has been reported that in dopaminergic neurons the firing rate and regularity of firing are under the control of SK channels (Iyer *et al.*, 2017). Thus, it is likely that the increased $[Ca^{2+}]_i$ induced by Abeta42 activates robust SK currents that regulate spontaneous firing and synaptic function of hippocampal networks (Lancaster & Adams, 1986; Stocker *et al.*, 1999). SK channels are of relevance for controlling various brain function like motor coordination (Walter *et al.*, 2006).

Abeta42 increases the probability of glutamate release and reduces the ability of NMDA synapses to sustain prolonged stimulation

The study of the effects of Abeta42 on *p* has been deeper investigated by measuring the paired pulse ratio (*PPR*) and the corresponding PPD. Hippocampal NMDA synapses are characterized by a net synaptic depression which can be regulated by either NMDARs desensitization (Mennerick & Zorumski, 1996) or activation of presynaptic $GABA_B$ receptors (Huang & Gean, 1994). This short-term synaptic plasticity slows down the firing rate of hippocampal network. To this regard, we have previously shown (Gavello *et al.*, 2018) that the spontaneous firing of cultured hippocampal neurons is characterized by bursts of APs of 600 ms duration at 50 Hz intraburst firing frequency,

that corresponds to an average time interval of 20 ms between APs. If we consider that Abeta42 significantly increases the PPD during 25 to 100 ms, we expect a consistent inhibition of AP firing with Abeta42, in agreement with the reduced number of bursts and burst duration detected by MEAs (Gavello *et al.*, 2018). This inhibitory effect is in line with what already observed in Tg2576 mice overexpressing Abeta peptides (Marcantoni *et al.*, 2014).

While our data reveal that Abeta42 increases the release probability (*p*) during paired pulses separated by 25 to 100 ms, it is evident that synapses treated with Abeta42 are unable to sustain prolonged stimulations during repetitive pulses at 10 Hz (Fig.6). This occurs if the increased *p* induced by the oligomers determines a rapid empty of vesicles, not followed by a fast replenishment as it occurs in hippocampal GABAergic interneurons after BDNF incubation (Baldelli et al., 2005). It should also be considered that the high frequency stimulation (10 Hz) used in our voltage-clamp experiments is 5-fold lower than the effective AP frequency measured by MEAs during the train of APs within a burst (50 Hz). This suggests that in more physiological conditions the effect of Abeta42 on NMDA synapses during fast and prolonged stimulation would be more pronounced in the overall firing inhibition.

Taken all together, we can conclude that the potentiating presynaptic effects of Abeta42 reported here strongly depend on the increased amount of Ca^{2+} released from RyRs. To this regard, the observation that dantrolene reverts the increased PPD induced by Abeta42 (Fig. 7) is in line with the previously reported effect of dantrolene that prevents the Abeta42-dependent increase of eEPSCs amplitude, the elevation of $[Ca^{2+}]_i$ and the inhibition of firing (Gavello *et al.*, 2018). This effective action of RyR inhibitors on glutamatergic synapses allows concluding that a pharmacological therapy based on the development of selective RyRs blockers have solid molecular basis to be tested.

Bibliography

Allio A, Calorio C, Franchino C, Gavello D, Carbone E & Marcantoni A. (2015). Bud extracts from Tilia tomentosa Moench inhibit hippocampal neuronal firing through GABAA and benzodiazepine receptors activation. *Journal of ethnopharmacology* **172,** 288-296.

Bacci A, Verderio C, Pravettoni E & Matteoli M. (1999). Synaptic and intrinsic mechanisms shape synchronous oscillations in hippocampal neurons in culture. *The European journal of neuroscience* **11,** 389-397.

Baldelli P, Hernandez-Guijo JM, Carabelli V & Carbone E. (2005). Brain-derived neurotrophic factor enhances GABA release probability and nonuniform distribution of N- and P/Q-type channels on release sites of hippocampal inhibitory synapses. *The Journal of neuroscience : the official journal of the Society for Neuroscience* **25,** 3358-3368.

Baldelli P, Novara M, Carabelli V, Hernandez-Guijo JM & Carbone E. (2002). BDNF up-regulates evoked GABAergic transmission in developing hippocampus by potentiating presynaptic N- and P/Q-type Ca2+ channels signalling. *The European journal of neuroscience* **16,** 2297-2310.

Bekkers JM & Stevens CF. (1989). NMDA and non-NMDA receptors are co-localized at individual excitatory synapses in cultured rat hippocampus. *Nature* **341,** 230-233.

Berridge MJ. (2011). Calcium signalling and Alzheimer's disease. *Neurochem Res* **36,** 1149-1156.

Chakroborty S, Briggs C, Miller MB, Goussakov I, Schneider C, Kim J, Wicks J, Richardson JC, Conklin V, Cameransi BG & Stutzmann GE. (2013). Stabilizing ER Ca2+ channel function as an early preventative strategy for Alzheimer's disease. *PloS one* **7,** e52056.

Chakroborty S, Goussakov I, Miller MB & Stutzmann GE. (2009). Deviant ryanodine receptor-mediated calcium release resets synaptic homeostasis in presymptomatic 3xTg-AD mice. *The Journal of neuroscience : the official journal of the Society for Neuroscience* **29,** 9458-9470.

Clements JD & Silver RA. (2000). Unveiling synaptic plasticity: a new graphical and analytical approach. *Trends in neurosciences* **23,** 105-113.

Costa RO, Lacor PN, Ferreira IL, Resende R, Auberson YP, Klein WL, Oliveira CR, Rego AC & Pereira CM. (2012). Endoplasmic reticulum stress occurs downstream of GluN2B subunit of N-methyl-d-aspartate receptor in mature hippocampal cultures treated with amyloid-beta oligomers. *Aging Cell* **11,** 823-833.

Danysz W & Parsons CG. (2012). Alzheimer's disease, beta-amyloid, glutamate, NMDA receptors and memantine--searching for the connections. *British journal of pharmacology* **167,** 324-352.

Dittman JS & Regehr WG. (1998). Calcium dependence and recovery kinetics of presynaptic depression at the climbing fiber to Purkinje cell synapse. *The Journal of neuroscience : the official journal of the Society for Neuroscience* **18,** 6147-6162.

Emptage N, Bliss TV & Fine A. (1999). Single synaptic events evoke NMDA receptor-mediated release of calcium from internal stores in hippocampal dendritic spines. *Neuron* **22,** 115-124.

Folch J, Busquets O, Ettcheto M, Sanchez-Lopez E, Castro-Torres RD, Verdaguer E, Garcia ML, Olloquequi J, Casadesus G, Beas-Zarate C, Pelegri C, Vilaplana J, Auladell C & Camins A. (2017). Memantine for the Treatment of Dementia: A Review on its Current and Future Applications. *Journal of Alzheimer's disease : JAD* **62,** 1223-1240.

Gavello D, Calorio C, Franchino C, Cesano F, Carabelli V, Carbone E & Marcantoni A. (2018). Early Alterations of Hippocampal Neuronal Firing Induced by Abeta42. *Cerebral cortex (New York, NY : 1991)* **28,** 433-446.

Gavello D, Rojo-Ruiz J, Marcantoni A, Franchino C, Carbone E & Carabelli V. (2012). Leptin counteracts the hypoxia-induced inhibition of spontaneously firing hippocampal neurons: a microelectrode array study. *PloS one* **7,** e41530.

Goussakov I, Miller MB & Stutzmann GE. (2010). NMDA-mediated Ca(2+) influx drives aberrant ryanodine receptor activation in dendrites of young Alzheimer's disease mice. *The Journal of neuroscience : the official journal of the Society for Neuroscience* **30,** 12128-12137.

Hoey SE, Williams RJ & Perkinton MS. (2009). Synaptic NMDA receptor activation stimulates alpha-secretase amyloid precursor protein processing and inhibits amyloid-beta production. *The Journal of neuroscience : the official journal of the Society for Neuroscience* **29,** 4442-4460.

Huang CC & Gean PW. (1994). Paired-pulse depression of the N-methyl-D-aspartate receptor-mediated synaptic potentials in the amygdala. *British journal of pharmacology* **113,** 1029-1035.

Iyer R, Ungless MA & Faisal AA. (2017). Calcium-activated SK channels control firing regularity by modulating sodium channel availability in midbrain dopamine neurons. *Scientific reports* **7,** 5248.

Jahr CE & Stevens CF. (1987). Glutamate activates multiple single channel conductances in hippocampal neurons. *Nature* **325,** 522-525.

Kim S, Yun HM, Baik JH, Chung KC, Nah SY & Rhim H. (2007). Functional interaction of neuronal Cav1.3 L-type calcium channel with ryanodine receptor type 2 in the rat hippocampus. *The Journal of biological chemistry* **282,** 32877-32889.

Kohr G, De Koninck Y & Mody I. (1993). Properties of NMDA receptor channels in neurons acutely isolated from epileptic (kindled) rats. *The Journal of neuroscience : the official journal of the Society for Neuroscience* **13,** 3612-3627.

Lacampagne A, Liu X, Reiken S, Bussiere R, Meli AC, Lauritzen I, Teich AF, Zalk R, Saint N, Arancio O, Bauer C, Duprat F, Briggs CA, Chakroborty S, Stutzmann GE, Shelanski ML, Checler F, Chami M & Marks AR. (2017). Post-translational remodeling of ryanodine receptor induces calcium leak leading to Alzheimer's disease-like pathologies and cognitive deficits. *Acta neuropathologica* **134,** 749-767.

Lambert MP, Barlow AK, Chromy BA, Edwards C, Freed R, Liosatos M, Morgan TE, Rozovsky I, Trommer B, Viola KL, Wals P, Zhang C, Finch CE, Krafft GA & Klein WL. (1998). Diffusible, nonfibrillar ligands derived from Abeta1-42 are potent central nervous system neurotoxins. *Proceedings of the National Academy of Sciences of the United States of America* **95,** 6448-6453.

Lancaster B & Adams PR. (1986). Calcium-dependent current generating the afterhyperpolarization of hippocampal neurons. *J Neurophysiol* **55,** 1268-1282.

Marcantoni A, Raymond EF, Carbone E & Marie H. (2014). Firing properties of entorhinal cortex neurons and early alterations in an Alzheimer's disease transgenic model. *Pflugers Archiv : European journal of physiology* **466,** 1437-1450.

Mattson MP. (2010). ER calcium and Alzheimer's disease: in a state of flux. In *Sci Signal*, pp. pe10. United States.

Mennerick S & Zorumski CF. (1996). Postsynaptic modulation of NMDA synaptic currents in rat hippocampal microcultures by paired-pulse stimulation. *The Journal of physiology* **490 (Pt 2),** 405-417.

Monyer H, Sprengel R, Schoepfer R, Herb A, Higuchi M, Lomeli H, Burnashev N, Sakmann B & Seeburg PH. (1992). Heteromeric NMDA receptors: molecular and functional distinction of subtypes. *Science (New York, NY)* **256,** 1217-1221.

Nimmrich V, Grimm C, Draguhn A, Barghorn S, Lehmann A, Schoemaker H, Hillen H, Gross G, Ebert U & Bruehl C. (2008). Amyloid beta oligomers (A beta(1-42) globulomer) suppress spontaneous synaptic activity by inhibition of P/Q-type calcium currents. *The Journal of neuroscience : the official journal of the Society for Neuroscience* **28,** 788-797.

Schneggenburger R, Sakaba T & Neher E. (2002). Vesicle pools and short-term synaptic depression: lessons from a large synapse. In *Trends in neurosciences*, pp. 206-212. England.

Shankar GM, Bloodgood BL, Townsend M, Walsh DM, Selkoe DJ & Sabatini BL. (2007). Natural oligomers of the Alzheimer amyloid-beta protein induce reversible synapse loss by modulating an NMDA-type glutamate receptor-dependent signaling pathway. *The Journal of neuroscience : the official journal of the Society for Neuroscience* **27,** 2866-2875.

Sigworth FJ. (1980). The variance of sodium current fluctuations at the node of Ranvier. *The Journal of physiology* **307,** 97-129.

Silver RA, Momiyama A & Cull-Candy SG. (1998). Locus of frequency-dependent depression identified with multiple-probability fluctuation analysis at rat climbing fibre-Purkinje cell synapses. *The Journal of physiology* **510 (Pt 3),** 881-902.

Snyder EM, Nong Y, Almeida CG, Paul S, Moran T, Choi EY, Nairn AC, Salter MW, Lombroso PJ, Gouras GK & Greengard P. (2005). Regulation of NMDA receptor trafficking by amyloid-beta. *Nature neuroscience* **8,** 1051-1058.

Stocker M, Krause M & Pedarzani P. (1999). An apamin-sensitive Ca2+-activated K+ current in hippocampal pyramidal neurons. *Proceedings of the National Academy of Sciences of the United States of America* **96,** 4662-4667.

Stutzmann GE, Caccamo A, LaFerla FM & Parker I. (2004). Dysregulated IP3 signaling in cortical neurons of knock-in mice expressing an Alzheimer's-linked mutation in presenilin1 results in exaggerated Ca2+ signals and altered membrane excitability. In *The Journal of neuroscience : the official journal of the Society for Neuroscience*, pp. 508-513. United States.

Thibault O, Pancani T, Landfield PW & Norris CM. (2012). Reduction in neuronal L-type calcium channel activity in a double knock-in mouse model of Alzheimer's disease. *Biochimica et Biophysica Acta (BBA) - Molecular Basis of Disease* **1822,** 546-549.

Traynelis SF & Jaramillo F. (1998). Getting the most out of noise in the central nervous system. *Trends in neurosciences* **21,** 137-145.

Walter JT, Alvina K, Womack MD, Chevez C & Khodakhah K. (2006). Decreases in the precision of Purkinje cell pacemaking cause cerebellar dysfunction and ataxia. *Nature neuroscience* **9,** 389-397.

Wang Y & Mattson MP. (2013). L-type Ca2+ currents at CA1 synapses, but not CA3 or dentate granule neuron synapses, are increased in 3xTgAD mice in an age-dependent manner. *Neurobiology of aging* **35,** 88-95.

Zhang Y, Li P, Feng J & Wu M. (2016). Dysfunction of NMDA receptors in Alzheimer's disease. *Neurological sciences : official journal of the Italian Neurological Society and of the Italian Society of Clinical Neurophysiology* **37,** 1039-1047.

Zhao F, Li P, Chen SR, Louis CF & Fruen BR. (2001). Dantrolene inhibition of ryanodine receptor Ca2+ release channels. Molecular mechanism and isoform selectivity. *The Journal of biological chemistry* **276,** 13810-13816.

Additional information

Competing interests

All authors declare no competing interests.

Author contribution

A.M. designed and performed experiments. wrote the manuscript with input from all co-authors.

S.C., P.B. and G.C. performed and analysed electrophysiological experiments.

V.C, E.C. revised critically the manuscript and contributed to design the experiments

All authors have read and approved the final version of this manuscript and agree to be accountable for all aspects of the work in ensuring that questions related to the accuracy or integrity of any part of the work are appropriately investigated and resolved. All persons designated as authors qualify for authorship.

Funding

This work was supported by the following projects: Project 2015FNWP34 (from Italian MIUR) to VC and AM, CSTO165284 (from Compagnia di San Paolo) to VC. Local funds from Torino University to AM, FFABR funds (Fondo Finanziamento delle Attività Base di Ricerca) from Italian MIUT to AM.

Acknowledgements

We are grateful to Dr. Claudio Franchino for the preparation of cell cultures.

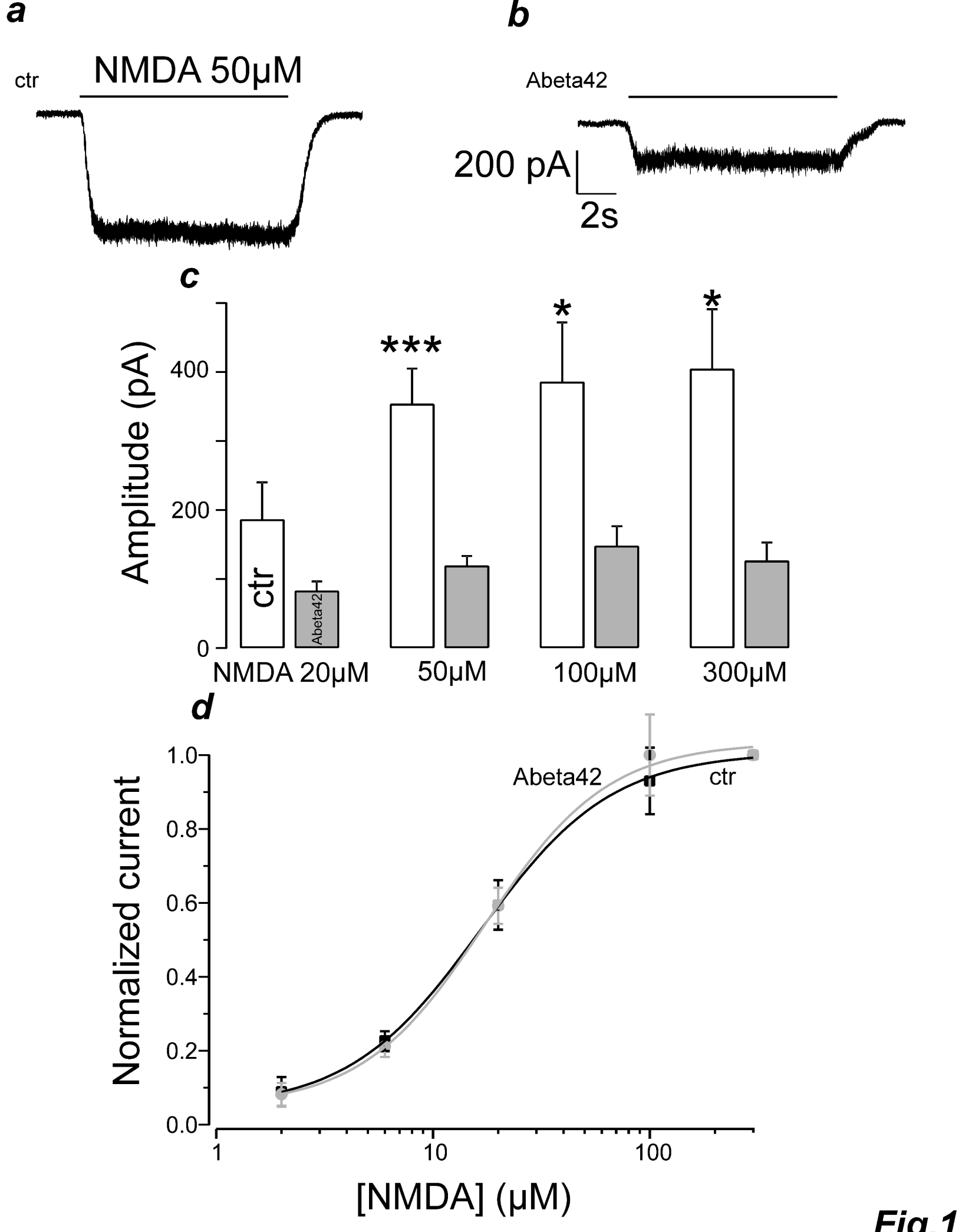
a
ctr
NMDA 50μM
b
Abeta42
200 pA
2s
c
Amplitude (pA)
400
200
0
ctr
Abeta42
***
*
*
NMDA 20μM
50μM
100μM
300μM
d
Normalized current
1.0
0.8
0.6
0.4
0.2
0.0
Abeta42
ctr
1
10
100
[NMDA] (μM)

Fig.1

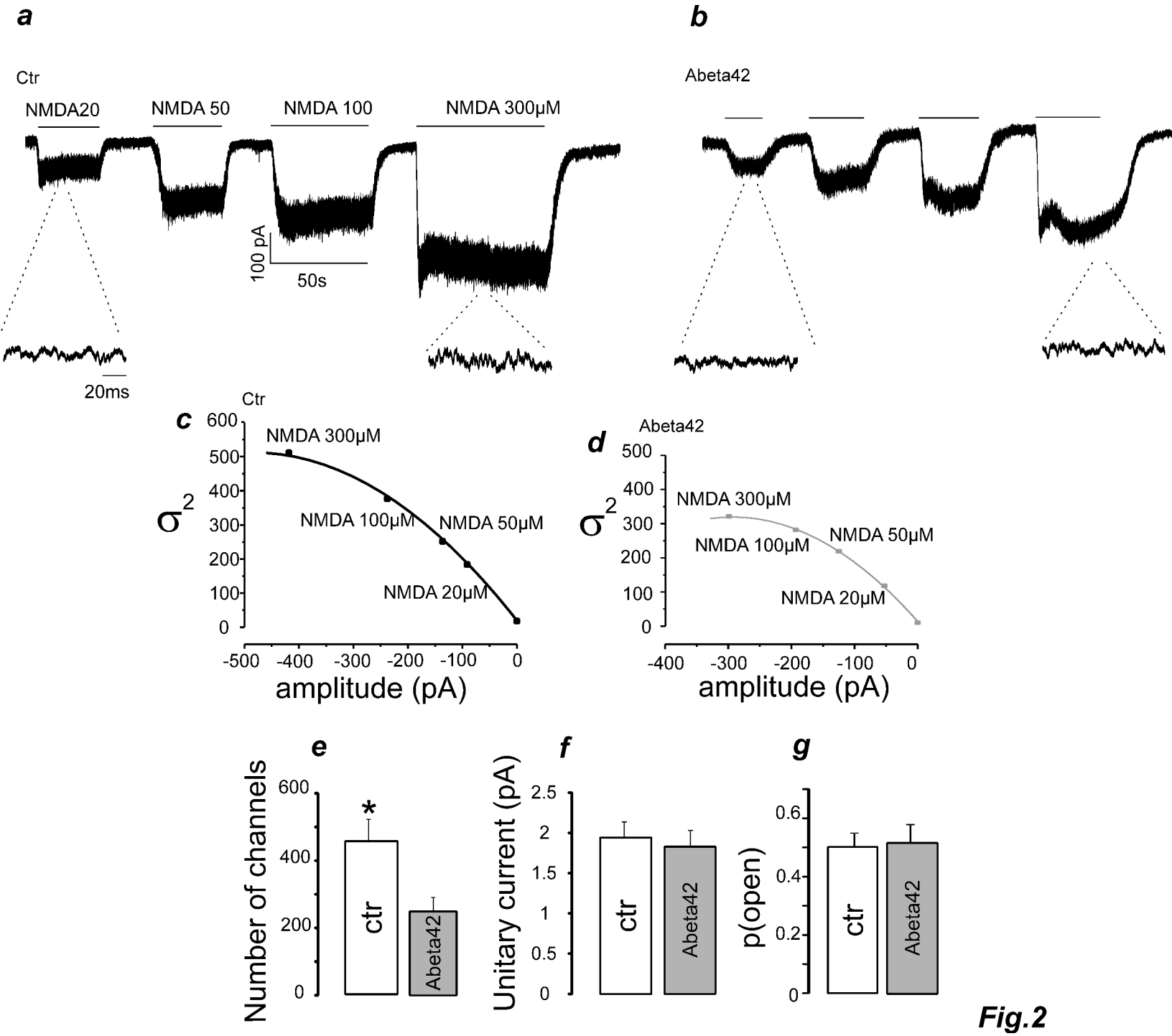
a
Ctr
NMDA20
NMDA 50
NMDA 100
NMDA 300μM
100 pA
50s
20ms
b
Abeta42
c
Ctr
NMDA 300μM
NMDA 100μM
NMDA 50μM
NMDA 20μM
σ2
amplitude (pA)
d
Abeta42
NMDA 300μM
NMDA 100μM
NMDA 50μM
NMDA 20μM
σ2
amplitude (pA)
e
Number of channels
ctr
Abeta42
*
f
Unitary current (pA)
ctr
Abeta42
g
p(open)
ctr
Abeta42

Fig.2

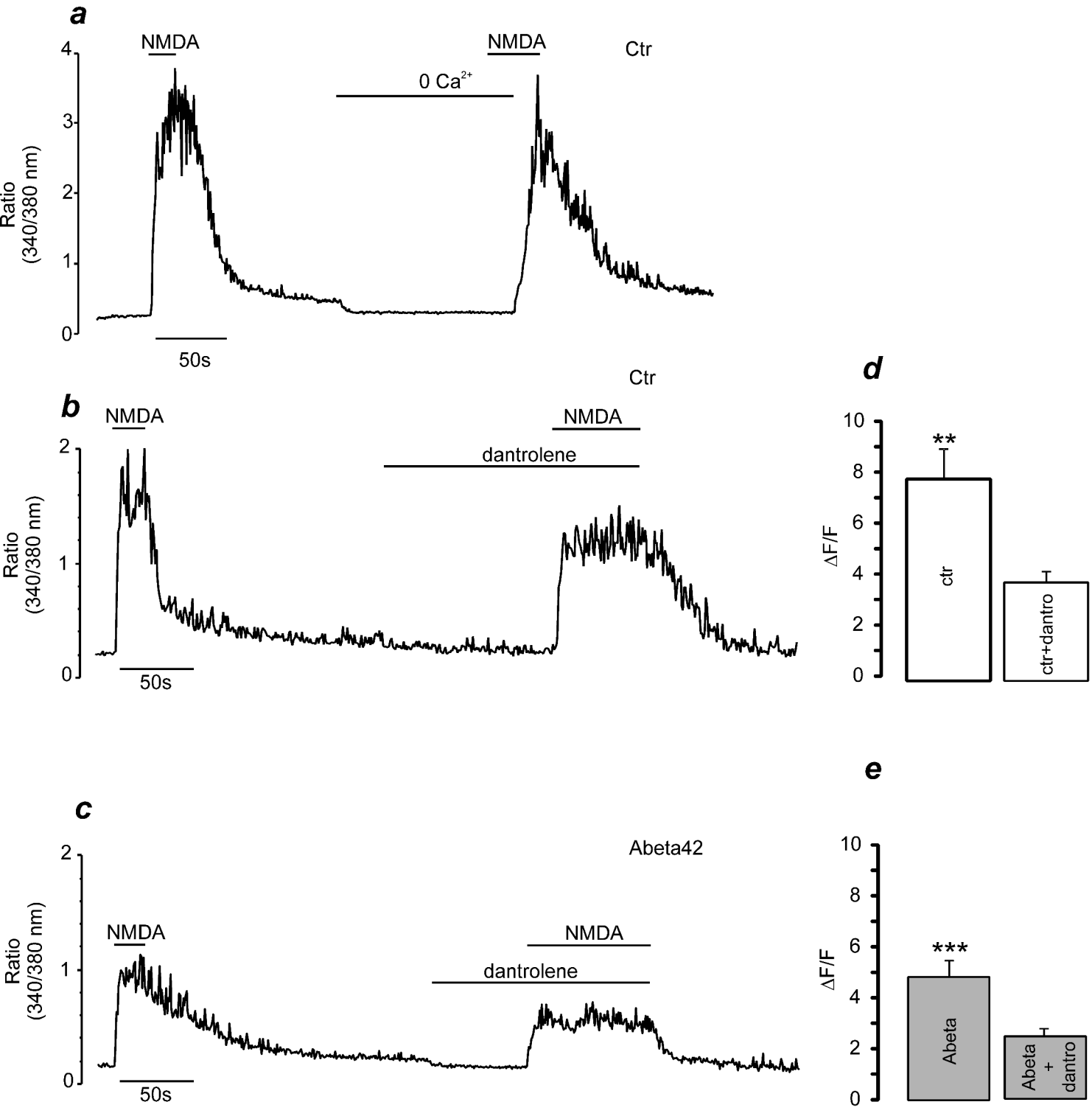
a
NMDA
NMDA
Ctr
0 Ca2+
Ratio (340/380 nm)
50s
b
Ctr
NMDA
NMDA
dantrolene
Ratio (340/380 nm)
50s
c
Abeta42
NMDA
NMDA
dantrolene
Ratio (340/380 nm)
50s
d
ΔF/F
**
ctr
ctr+dantro
e
ΔF/F
***
Abeta
Abeta + dantro

Fig.3

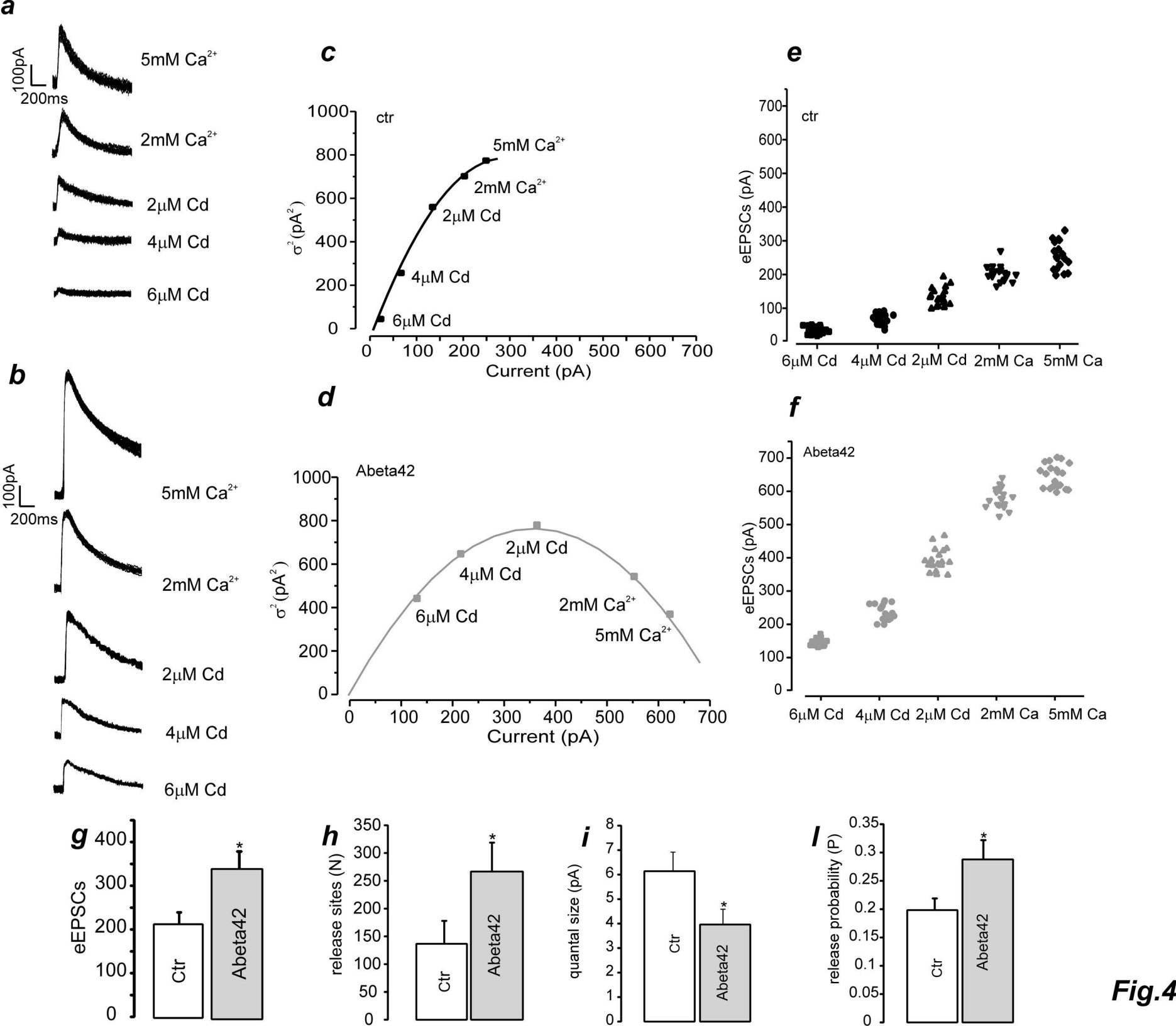
a
100pA
200ms
5mM Ca2+
2mM Ca2+
2μM Cd
4μM Cd
6μM Cd
b
100pA
200ms
5mM Ca2+
2mM Ca2+
2μM Cd
4μM Cd
6μM Cd
c
ctr
σ2 (pA2)
Current (pA)
5mM Ca2+
2mM Ca2+
2μM Cd
4μM Cd
6μM Cd
d
Abeta42
σ2 (pA2)
Current (pA)
2μM Cd
4μM Cd
6μM Cd
2mM Ca2+
5mM Ca2+
e
ctr
eEPSCs (pA)
6μM Cd
4μM Cd
2μM Cd
2mM Ca
5mM Ca
f
Abeta42
eEPSCs (pA)
6μM Cd
4μM Cd
2μM Cd
2mM Ca
5mM Ca
g
eEPSCs
Ctr
Abeta42
h
release sites (N)
Ctr
Abeta42
i
quantal size (pA)
Ctr
Abeta42
l
release probability (P)
Ctr
Abeta42

Fig.4

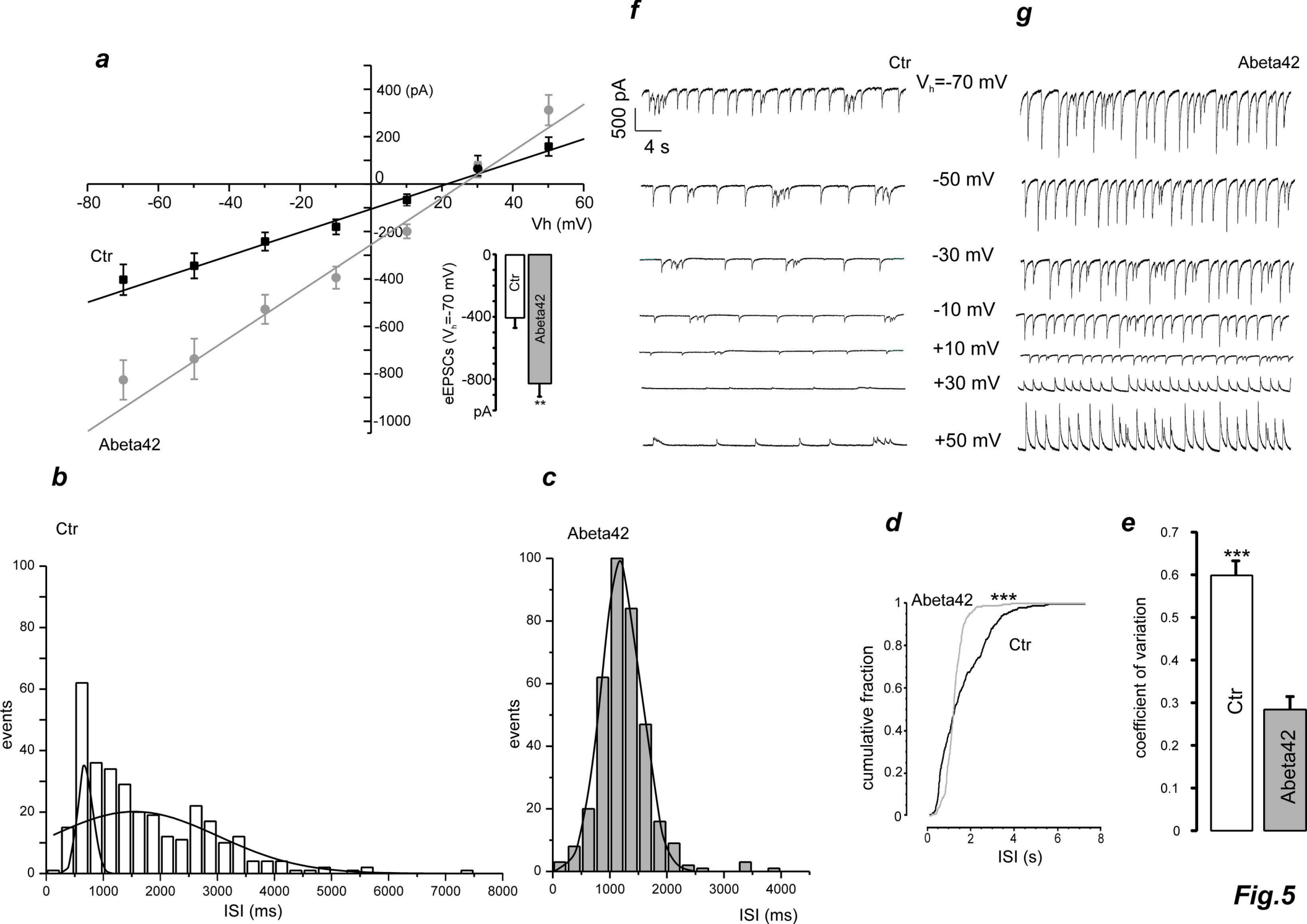
a
400 (pA)
200
0
-200
-400
-600
-800
-1000
-80
-60
-40
-20
20
40
60
Vh (mV)
Ctr
Abeta42
eEPSCs (Vh=-70 mV)
0
-400
-800
pA
Ctr
Abeta42
**
f
Ctr
500 pA
4 s
Vh=-70 mV
-50 mV
-30 mV
-10 mV
+10 mV
+30 mV
+50 mV
g
Abeta42
b
Ctr
events
ISI (ms)
c
Abeta42
events
ISI (ms)
d
Abeta42
***
Ctr
cumulative fraction
ISI (s)
e
***
coefficient of variation
Ctr
Abeta42

Fig.5

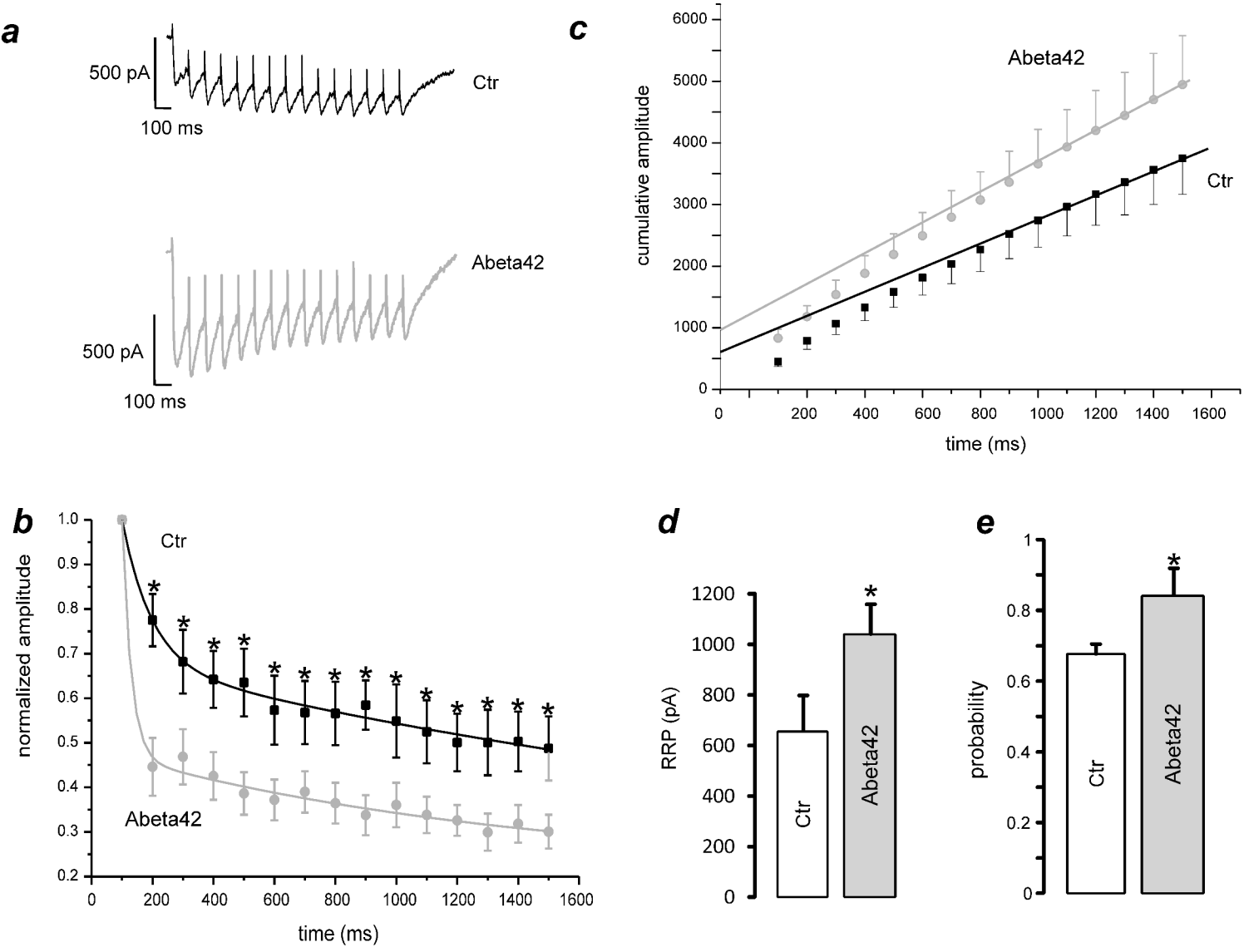
a
500 pA
100 ms
Ctr
Abeta42
500 pA
100 ms
c
cumulative amplitude
Abeta42
Ctr
time (ms)
b
normalized amplitude
Ctr
Abeta42
time (ms)
d
RRP (pA)
Ctr
Abeta42
e
probability
Ctr
Abeta42

Fig.6

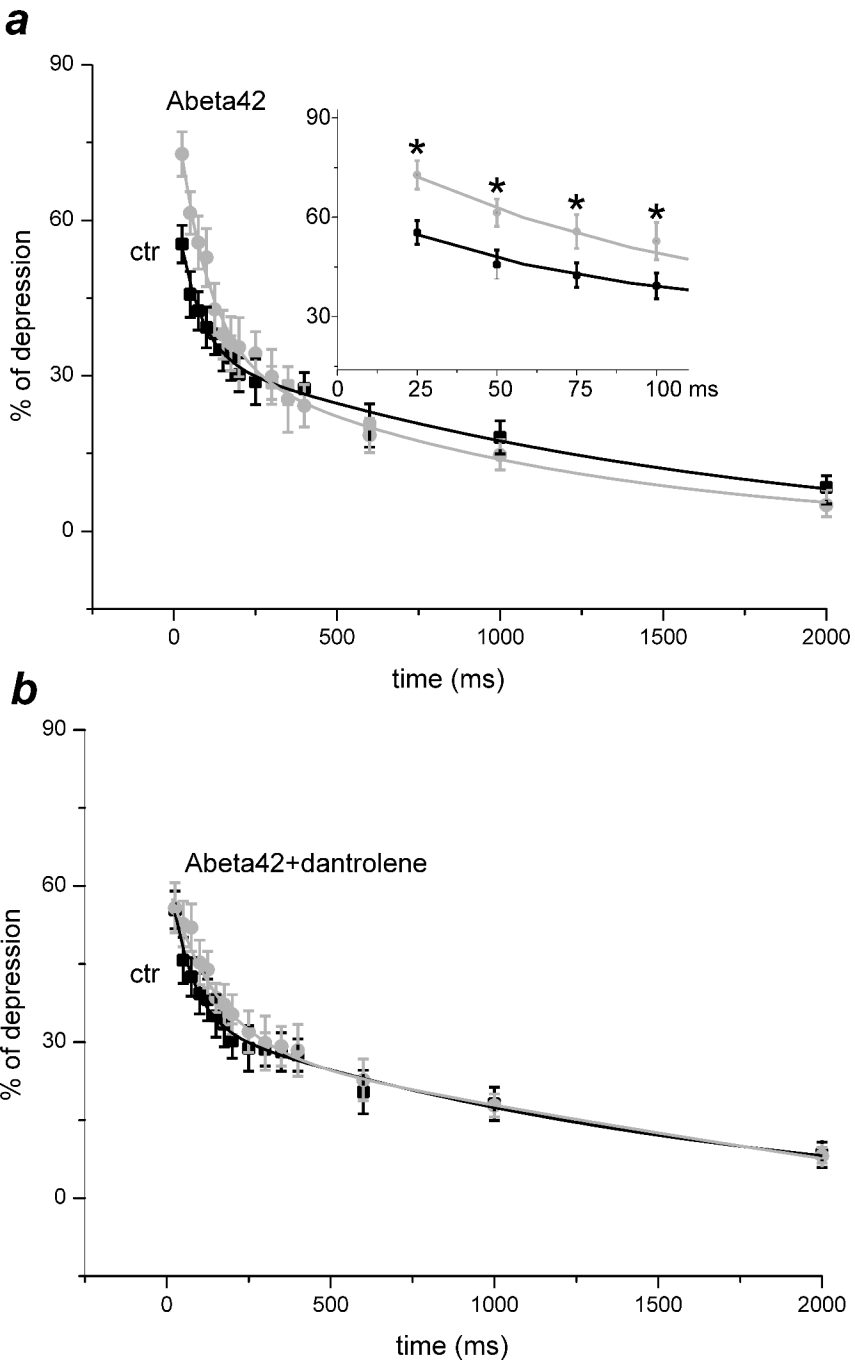
a
Abeta42
ctr
% of depression
time (ms)
b
Abeta42+dantrolene
ctr
% of depression
time (ms)
c
25 ms
100 ms
ctr
100 pA
100 ms
d
Abeta42
e
Abeta42+dantrolene

Fig.7

Figures legend

Fig.1

a) Representative inward current activated by NMDA (50μM) recorded in patch clamp experiment on primary cultured hippocampal neurons by holding neurons at V_h=-70mV. **b**) When neurons are incubated for 48h with Abeta42 the current activate by NMDA administration is significantly inhibited. **c**) Bar graphes summarizing the inhibitory effect induced by Abeta42 on inward currents activated by different concentrations of NMDA (from 20 to 300 μM). **d**) The dose response sigmoid curve of the current activated by NMDA (from 2 to 300 μM) is not affected by Abeta42.

Fig.2

a) In control neurons NMDA administration activates inward currents of increased amplitude depending by the increased concentration of the agonist (from 20 to 300 μM). The insets show the noise signal that increases together with the increased current amplitudes. **b**) Abeta42 decreases the amplitude of inward currents activated by increasing concentrations of NMDA as well as the noise signal. **c**) Representative parabolic relationship between the variance (σ^2) of noise signal and mean of the inward current activated by NMDA at different concentrations in control neurons and in the presence of Abeta42 (**d**). **e**) Bar graph summarizing the significant decrease of the average number of NMDARs induced by Abea42, despite their unitary current (**f**) and open probability (**g**) remain unchanged.

Fig.3

a) In calcium imaging experiments performed in control neurons NMDA (50μM) increases $[Ca^{2+}]_i$ when neurons are perfused with extracellular Tyrode standard solution containing 2mM Ca^{2+}, while this effect is reversibly abolished in the absence of Ca^{2+} (0 Ca^{2+}) in the extracellular medium. **b**) In control neurons the inhibition of RyRs through dantrolene (10 μM) halved the effect induced by NMDA. **c**) Abeta42 reduced by 50% the effect induced by NMDA on $[Ca^{2+}]_i$ and, similarly to control neurons, dantrolene halved the effect induced by NMDA. **d**) Bar graph summarizing the effect induced by NMDA (50μM) on $[Ca^{2+}]_i$ in control neurons and the related contribution of RyRs estimated by administration of dantrolene. **e**) Similarly to (d) the bar graph summarizes the effect induced by NMDA (50μM) on $[Ca^{2+}]_i$ in the presence of Abeta42

Fig.4

a) Thirty overlapped eEPSCs traces dependent by NMDARs activation recorded in control neurons under different release probability conditions recorded by varying the concentrations of $CaCl_2$ or $CdCl_2$ in the external medium in order to change the release probability conditions. **b**) Thirty overlapped eEPSCs traces recorded after incubation of neurons with Abeta42 under different release probability conditions similarly to what shown in (a). **c**) Parabolic distribution of σ^2 in function of eEPSCs amplitude recorded in control neurons. **d**) Parabolic distribution of σ^2 in function of eEPSCs amplitude recorded in neurons incubated with Abeta42. **e**) Peak amplitude of eEPSCs recorded in control neurons in function of different concentrations of cadmium or calcium in the external medium **f**) Peak amplitude of eEPSCs recorded in neurons incubated with Abeta42 in function of different concentrations of cadmium or calcium in the external medium. **g**) Bar graph of the average amplitude of eEPSCs recorded at +20mV with 2mM Ca^{2+} in the external medium, **h**) of the number of release sites, **i**) of the quantal size, and **l**) of the release probability of NMDA synapses in control neurons and in the presence of Abeta42.

Fig.5

a) Mean EPSCs amplitude evoked by spontaneous action potentials measured in control neurons and after administration of Abeta42 by holding neurons at membrane potentials comprised between -70 and +50 mV. **b**, **c**) Spontaneous EPSCs recorded in control neuron and in the presence of Abeta42 by holding neurons at membrane potentials comprised between -70 and + 50 mV. **d**, **e**) Histograms showing the distribution of EPSCs in function of inter event intervals (IEI) in control neurons and in the presence of Abeta42. **f**) Cumulative IEIs distribution of spontaneous EPSCs in control neurons and in neurons incubated with Abeta42. **g**) Bar graph of the coefficient of variation of IEIs in control neurons and in the presence of Abeta42.

Fig.6

a) eEPSCs recorded in control (top, black) and Abeta42 (bottom, grey) treated neurons by delivering repetitive constant pulses of current at 10Hz for 1.5 s. **b**) Normalized eEPSCs amplitude in function of time. **c**) Cumulative amplitude distribution of eEPSCs in function of time in control and after incubation of neurons with Abeta42. The final portion of the distribution follows a linear distribution. The intercept of the linear fit with y-axes provides a quantification of RRP size. **d**, **e**) Bar graphs of the size of RRP and release probability in control neurons and in neurons treated with Abeta42.

Fig.7

a) Mean PPD (Paired Pulse Depression) values plotted in function of IEIs of different duration (comprised between 25 and 2000 ms). The inset shows at higher magnification the PPD values calculated for IEIs between 25 and 100ms. **b**) mean PPD values recorded after administration of dantrolene to neurons incubated with Abeta42. **c-e**) Paired eEPSCs recorded by setting the IEI at 25 and 100 ms in control neurons (c), in neurons treated with Abeta42 (d) and in neurons treated with Abeta42 together with dantrolene (e).